Thermal analysis of selected Sn–Ag–Cu alloys

Przemysław Fima · Andrzej Gazda

Abstract The phase transitions proceeding during melting of selected Sn–Ag–Cu alloys were determined by means of the DSC technique. Twelve compositions were studied along two cross-sections with silver to copper molar ratios $X(Ag)/X(Cu) = 1$ and 7/3 and tin concentration from 0.4 to 0.9 mol fraction. The transition temperatures were calculated using Pandat software package and thermodynamic parameters from the SOLDERS database. The experimental results were compared with both available literature data and calculation results, and a good agreement was observed. Deconvolution of DSC complex curves was performed using PeakFit v.4.12 software package. Eutectic mixture mass fractions involved in the eutectic transformation were determined. The obtained results were compared with the data calculated using thermodynamic parameters and good agreement was achieved in the case of alloys of higher content of Sn. The discrepancy was found in the case of alloys with lower Sn content where initial structure of the samples subjected to DCS analysis was partly a result of the occurrence of peritectic transformation.

P. Fima (✉)
Institute of Metallurgy and Materials Science, Polish Academy of Sciences, 25 Reymonta St., 30-059 Krakow, Poland
e-mail: nmfima@imim-pan.krakow.pl

P. Fima · A. Gazda
Center for High-Temperature Studies, Foundry Research Institute, 73 Zakopianska St., 30-418 Krakow, Poland

Introduction

The first order phase transformations proceeding in solid and liquid states are characterized by non-zero volume and entropy (or enthalpy) changes. On that reason, one of the thermal analysis (TA) methods—differential scanning calorimetry (DSC)—is suitable and very useful for the examination of metals and alloys in solid and liquid states. DSC enables analysis of phase transformations, yields data required to prepare phase diagrams and provides quantitative information about the kinetics of phase transformations [1, 2].

The Sn–Ag–Cu ternary system has been a subject of interest and intensive research for more than 15 years [3]. The main reason is, tin-rich alloys based on this system can be used as lead-free solders [4]. There is a number of works regarding TA of Sn–Ag–Cu alloys [3, 5–16] but complex analysis of melting and solidification characteristics in a wide range of temperatures and concentrations is still missing. Most of these works concentrate on tin-rich corner of Sn–Ag–Cu system. For example, Moon et al. [5] studied Sn-rich corner of the Sn–Ag–Cu system to find eutectic composition and temperature to be at 3.5 wt% Ag, 0.9 wt% Cu, and 217.2 °C, respectively. The findings of Loomans and Fine [6] agree with that very well. For a broader composition range, recently Marianovic et al. [16] using differential thermal analysis (DTA) studied invariant reactions for three cross-sections of constant molar ratios $X(Ag)/X(Cu) = 1$, $X(Ag)/X(Sn) = 1$, $X(Cu)/X(Sn) = 1$, four compositions each, every 0.2 mol fractions of the third component. Utilizing thermodynamic parameters from the SOLDERS database [17], they calculated phase diagram cross-sections and liquidus projection. They obtained relatively good agreement between calculated and experimentally determined invariant reactions for most of the

compositions they studied [16]. Thermodynamic data available in the SODERS database [17], developed under the framework of COST Action 531, come from an assessment partially based on previous studies of phase equilibria in the Sn–Ag–Cu ternary system. For reasons stated above, it is interesting to reinvestigate this system using different technique, starting from Sn-rich corner.

It is noticeable lack of comprehensive, calorimetric study aimed in applying of DSC technique to determine the specific enthalpy changes of separate phase transformation proceeding in Sn–Ag–Cu system, especially for alloys with non-eutectic compositions. The main goal of this work is to enhance available data on phase transitions in the Sn–Ag–Cu ternary alloys that can be used for better thermodynamic description of this system.

Experimental

Twelve compositions in Sn–Ag–Cu ternary were studied along two cross-sections of constant silver to copper molar ratios $X(Ag)/X(Cu) = 1$ and 7/3 and tin concentrations $X(Sn) = 0.9, 0.8, 0.7, 0.6, 0.5, 0.4$, respectively. Before starting with ternary samples, preliminary measurements on selected compositions from Sn–Ag ($X(Ag) = 0.1; 0.2; 0.3; 0.5$), Sn–Cu ($X(Cu) = 0.1; 0.2; 0.3; 0.5$), and Ag–Cu ($X(Ag) = 0.3; 0.4; 0.5$) binaries were carried out.

The alloys were prepared by melting accurately weighted amounts of pure elements (Sn 99.999 %, Ag 99.99 %, Cu 99.999 %) to obtain alloys of desired composition. Alloys were melted in graphite crucibles under protective atmosphere of high purity Ar (99.9999 %) to ensure that no oxidation occurred during melting process. The investigations were carried out using differential scanning calorimeter Netzsch DSC 404 C Pegasus. Before realizing the DSC experiments, the sensitivity and temperature calibration of DSC were performed by measuring the heat of melting and the melting temperature, respectively, of pure elements (In, Sn, Bi, Zn, Al and Ag) using the same working conditions. The samples ca 50 mg were ultrasonically cleaned in acetone and placed in the alumina crucibles of DSC holder. They were heated at a relatively low rate of 5 K min^{-1} in argon (99.9999 %) protective atmosphere and DSC curves were recorded.

Solidus, liquidus, and other characteristic temperatures can be determined by analyzing the thermal effects revealing in DSC curves. Extrapolated onset temperature was established as a measure of invariant reaction temperature; this parameter does not depend significantly on the experimental heating rate. To estimate liquidus temperature the peak maximum or extrapolated end temperature can be chosen. In the case of complex (non-eutectic) effects and higher heating rates, the temperature maximum

of the last peak was considered because of relatively weak dependence of this parameter on the heating rate [7]. Figure 1 shows exemplary DSC curves of alloys Sn–Cu and Sn–Ag–Cu with thermal effects evoked by heating of the alloy. The DSC curves maintain their complex nature over the experimental temperature range. The overlapping effects which can be found in DSC curves at higher temperature make the qualitative analysis difficult.

In the solidus–liquidus temperature range (Fig. 1), bulk thermal effect ΔH of melting process can be determined as the area limited by DSC curve and baseline divided by the
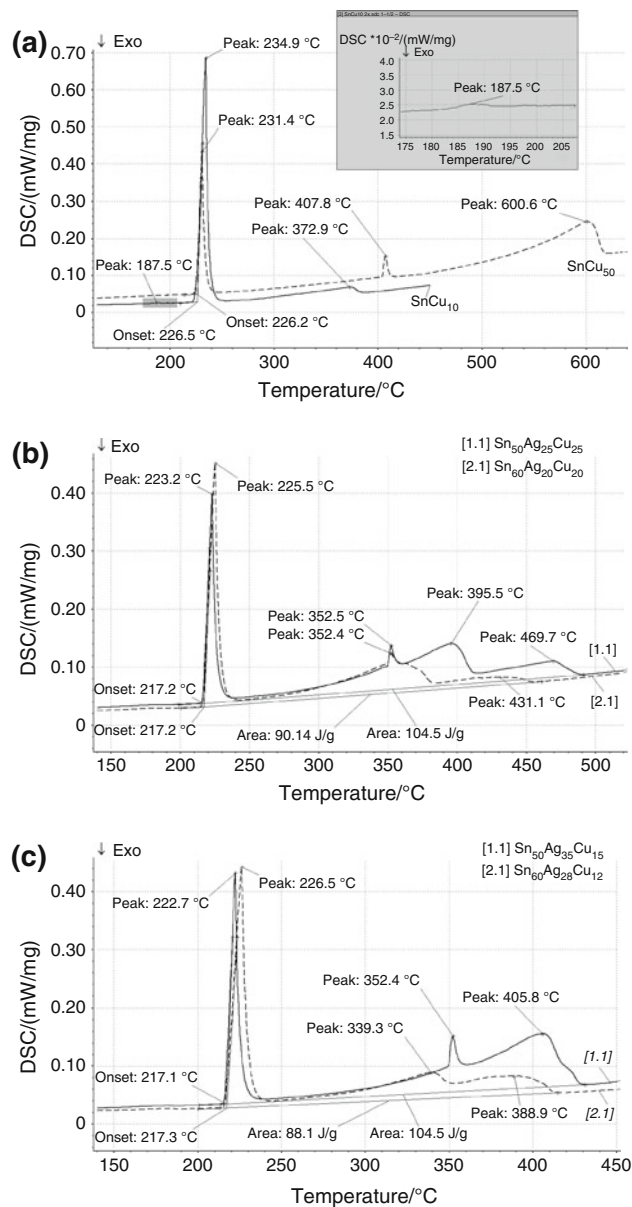

Fig. 1 DSC curves of alloys (in at%): **a** Sn$_{10}$Cu (*continuous line*) and Sn$_{50}$Cu (*dashed line*), **b** Sn$_{50}$Ag$_{25}$Cu$_{25}$ (*continuous line*) and Sn$_{60}$Ag$_{20}$Cu$_{20}$ (*dashed line*), **c** Sn$_{50}$Ag$_{35}$Cu$_{15}$ (*continuous line*) and Sn$_{60}$Ag$_{28}$Cu$_{12}$ (*dashed line*)

total mass m of specimen. Deconvolution of complex DSC curve enables separation of proceeding consecutively phase transitions, reflected as DSC peaks. Determination of their shares $u_1 \ldots u_k \ldots u_n$ i.e. shares in the total measured thermal effect allows to calculate the specific enthalpy changes ΔH_s^k related to the mass change of substrates or products engaged in kth transition, according to the formula:

$$\Delta H_s^k = \frac{u_k \Delta H}{f w_k} \tag{1}$$

or

$$f w_k = u_k \frac{\Delta H}{\Delta H_s^k} \tag{2}$$

where $f w_k$ denotes the resulting change of mass fraction of substance transformed.

Results

The experimental phase transition temperatures and bulk thermal effects for Sn–Ag, Sn–Cu and Ag–Cu alloys are collected in Table 1, and compared graphically in Fig. 2 against phase diagrams calculated based on thermodynamic data from the SOLDERS database [17]. The enlarged section of Fig. 1 shows the solid-state allotropic transformation $Cu_6Sn_5 \leftrightarrow Cu_6Sn_5$ occurring below the solidus at approximately 180 °C, characterized by very small endothermic effect, indistinguishable in normal drawing scale. In Cu–Sn alloys, two invariant reactions, eutectic reaction $(Sn) + Cu_6Sn_5 \leftrightarrow L$ and the peritectic reaction $Cu_6Sn_5 \leftrightarrow L + Cu_3Sn$ occurring only in alloys containing more than 10 at% of Cu, were found. In general, very good agreement is observed between the measured

and the calculated phase transition temperatures. This suggests that results for ternary alloys can be of high accuracy.

Eutectic reaction $(Sn) + Ag_3Sn + Cu_6Sn_5 \leftrightarrow L$ occurring at 217.2 ± 0.2 °C was found in all of the investigated ternary alloys, while the peritectic reaction $Cu_6Sn_5 + Ag_3Sn \leftrightarrow L + Cu_3Sn$ proceeding at 350.1 ± 0.3 °C was recorded only in alloys containing no more than 60 at% of Sn. The temperatures of phase transformations and bulk thermal effects, obtained from the DSC measurements of ternary alloys are collected in Table 2. The results of measurements are compared in Fig. 3 with the cross-sections calculated with the Pandat package using thermodynamic description of Sn–Ag–Cu system from SOLDERS database [17]. A comparison of calculated and experimentally determined temperatures of invariant reactions shows generally good agreement between them. The solid-state allotropic reaction occurring below the solidus at ~ 180 °C was confirmed for both cross-sections. Since there is no such reaction in Sn–Ag binary, in future studies of Sn–Ag–Cu ternary it would be interesting to find how high must be silver to copper ratio for this line to disappear.

The determined solidus line in the range $X(Sn) > 0.4$ (corresponding to eutectic reaction) is in very good agreement with the calculated one, also the majority of the remaining experimentally determined solid-state reactions show a close match to the results of calculations. The experimentally determined liquidus of $Sn_{70}Ag_{15}Cu_{15}$ (at%) alloy is higher than it was expected according to calculations. According to calculations and experimental data, for $X(Ag)/X(Cu) = 7/3$, the distance between the liquidus and a line representing the nearest reaction occurring below is smaller compared to $X(Ag)/X(Cu) = 1$. A comparison of our results for $X(Ag)/X(Cu) = 1$ cross-section with the DTA data from [16] indicate that using the DSC technique,

Table 1 Results of DSC analysis of selected binary Sn–Ag, Sn–Cu, and Ag–Cu alloys

| Binary system	Sample composition/at%	Enthalpy change, ΔH/J g^{-1}	Phase transition temperature/°C		
			Invariant reaction	Other transition	Liquidus
Sn–Ag	$Sn_{90}Ag_{10}$	71.3	221.6		311.9
	$Sn_{80}Ag_{20}$	72.6	221.5		352.1
	$Sn_{70}Ag_{30}$	79.5	223.0		406.2
	$Sn_{50}Ag_{50}$	79.2	221.9		467.1
Sn–Cu	$Sn_{90}Cu_{10}$	67.4	230.5	188.2	397.8
	$Sn_{80}Cu_{20}$	74.7	227.0, 421.7	186.4	472.0
	$Sn_{70}Cu_{30}$	70.3	227.9, 412.8	188.2	520.4
	$Sn_{50}Cu_{50}$	105.6	226.7, 406.4	187.8	606.4
Ag–Cu	$Ag_{70}Cu_{30}$	103.1	780.1		819.9
	$Ag_{60}Cu_{40}$	114.6	778.7		
	$Ag_{50}Cu_{50}$	127.9	779.2		813.2

(a)

(b)

(c)
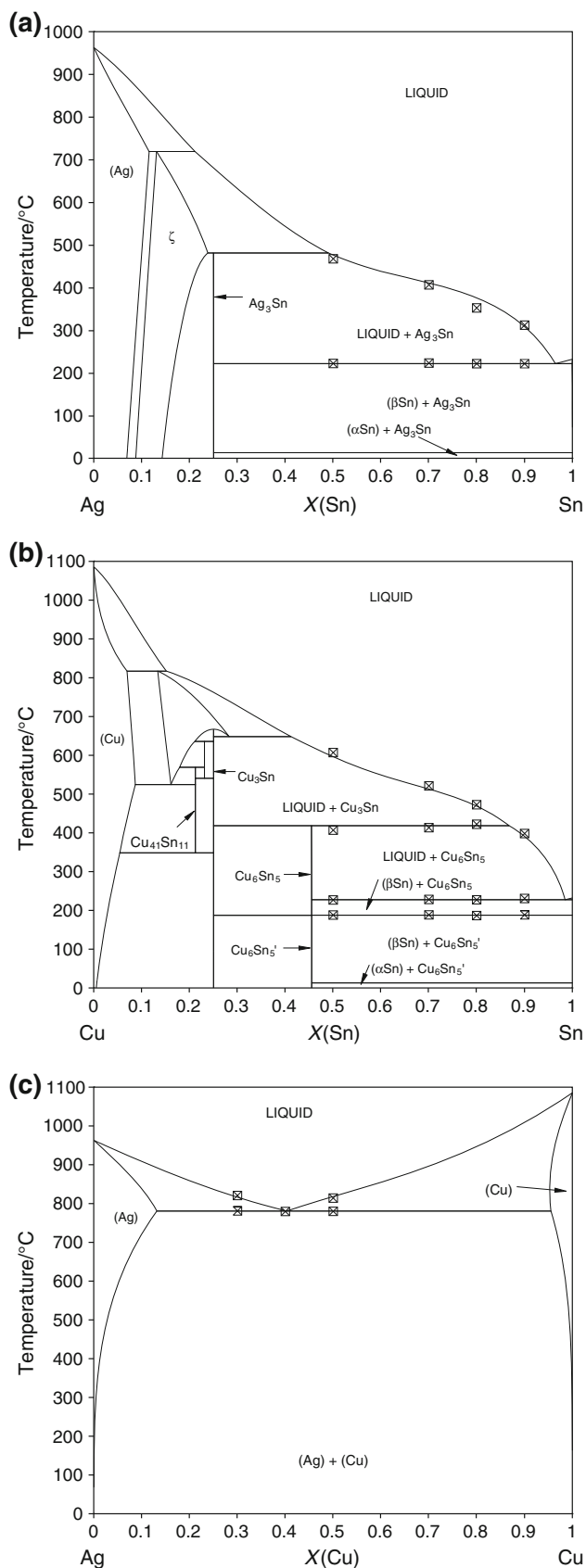
◄ **Fig. 2** The calculated phase diagrams compared with DSC results from the present study: **a** Sn–Ag, **b** Sn–Cu, **c** Ag–Cu. Calculations performed with Pandat based on thermodynamic data from SOL-DERS database [17], *crossed squares* correspond to transition temperatures listed in Table 1

we were able to confirm more of the invariant reactions at respective compositions, that are present according to calculations.

Discussion

Complex DSC curves consisting of the overlapping thermal effects in the solidus–liquidus temperature range can be separated by means of specialized software using analytical peak profiles and appropriate curve fitting methods. Figure 4 presents exemplary DSC curves of the $Sn_{40}Ag_{30}Cu_{30}$ alloy after deconvolution performed using PeakFit v.4.12. The upper curve shows experimental data (open circles) and the analytical curves fit; the lower curve demonstrates the separated peaks. This analytical solution provides the shares $u_1 \ldots u_k \ldots u_n$ of separated phase transitions in the bulk, and measured thermal effect ΔH.

Two invariant reactions (see Table 2), namely: eutectic $(Sn) + Ag_3Sn + Cu_6Sn_5 \leftrightarrow L$ and peritectic $Cu_6Sn_5 + Ag_3Sn \leftrightarrow L + Cu_3Sn$ were initially considered. However, thermal effects associated with the peritectic reaction were not analyzed further because of the small number of data and very low intensity peaks, which could result in large

Table 2 Results of DSC measurement of the investigated Sn–Ag–Cu alloys

| Sample composition/ at%	Enthalpy change, ΔH/J g^{-1}	Phase transition temperature/°C		
		Invariant reaction	Other transition	Liquidus
$Sn_{40}Ag_{30}Cu_{30}$	96.9	216.8, 349.7	181.8, 433.7	525.4
$Sn_{50}Ag_{25}Cu_{25}$	104.5	217.4, 350.4	181.7, 395.4	469.7
$Sn_{60}Ag_{20}Cu_{20}$	90.1	217.2, 350.3	182.1	431.1
$Sn_{70}Ag_{15}Cu_{15}$	90.9	217.3,	181.0, 331.3, 361.7	412.3
$Sn_{80}Ag_{10}Cu_{10}$	83.4	217.2,	181.5, 300.7	354.3
$Sn_{90}Ag_5Cu_5$	70.2	217.4,	183.8	313.5
$Sn_{40}Ag_{42}Cu_{18}$	102.4	216.8, 350.0	178.4, 439.7	465.6
$Sn_{50}Ag_{35}Cu_{15}$	104.5	217.1, 350.1	183.8, 405.8	422.8
$Sn_{60}Ag_{28}Cu_{12}$	88.1	217.3, 350.1	181.5, 339.3	388.9
$Sn_{70}Ag_{21}Cu_9$	91.2	217.1	181.8	347.5
$Sn_{80}Ag_{14}Cu_6$	81.6	217.3	184.2, 293.0	318.0
$Sn_{90}Ag_7Cu_3$	74.9	217.5	180.0	255.0
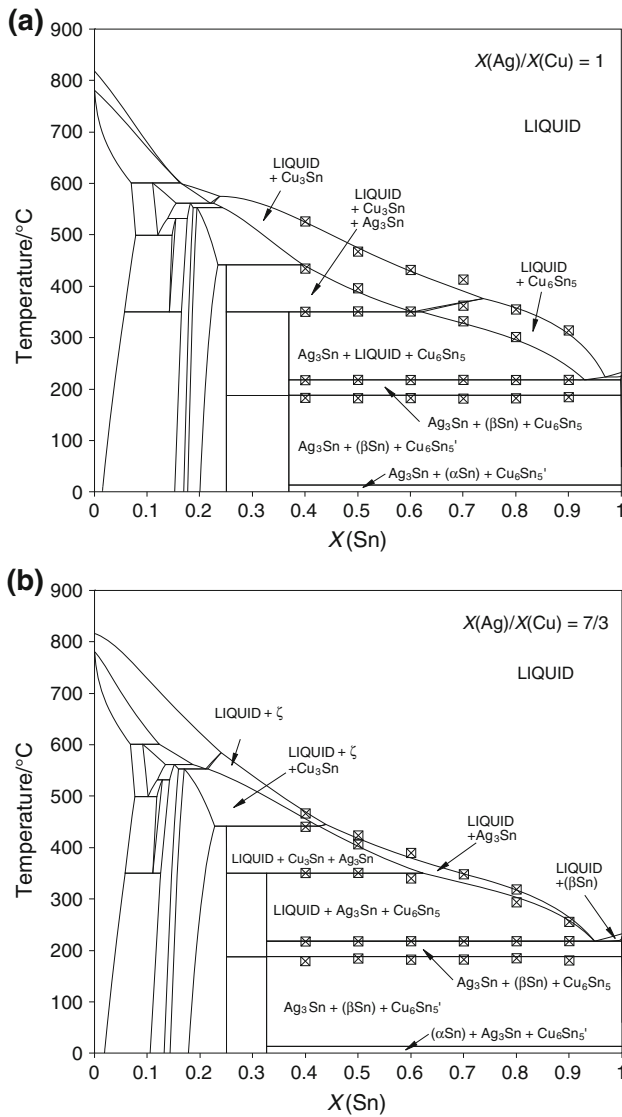
Fig. 3 The calculated phase diagrams compared with DSC results from the present study for two cross-sections in the Sn–Ag–Cu ternary system: **a** $X(Ag)/X(Cu) = 1$; **b** $X(Ag)/X(Cu) = 7/3$. Calculations performed with Pandat based on thermodynamic data from SOLDERS database [17], *crossed squares* correspond to transition temperatures listed in Table 2

Fig. 4 Exemplary deconvolution of DSC curve of alloy $Sn_{40}Ag_{30}Cu_{30}$ (at%). *Upper figure* experimental DSC curve, *lower figure* separated peaks

Fig. 5 DSC curve of the eutectic alloy $Sn_{96.0}Ag_{3.1}Cu_{0.9}$ (at%) recorded on heating (*continuous line*) and cooling (*dashed line*)

errors in the estimated contribution (u_k) of these effects in the whole transformation.

Analysis of eutectic transformation in ternaries was supported by the additional DSC analysis of some SAC305 alloys of eutectic composition; a criterion to qualify as an alloy of eutectic composition has been the lack of hypoeutectic primary phases registered on both the heating and cooling DSC curves. Figure 5 presents DSC curve recorded for the selected alloy of eutectic composition $Sn_{96.0}Ag_{3.1}Cu_{0.9}$ at%, provided by Alpha Metals Loetsysteme GmbH. Enlarged detail of DSC curve confirms the lack of hypoeutectic transformations. The measured specific enthalpy change accompanying the eutectic
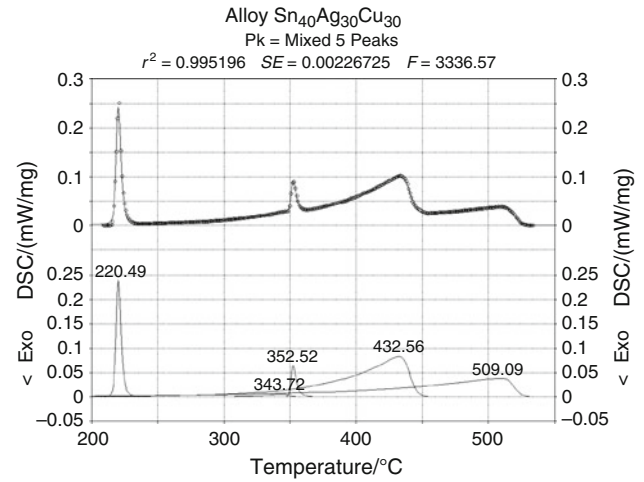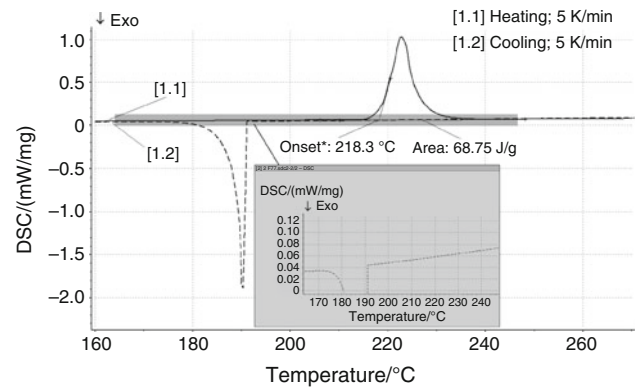
transformation in eutectic system equals 67.8 ± 2.1 J g^{-1}. For all the investigated alloys, taking this constant value of enthalpy change as ΔH_s^k, the bulk thermal effects ΔH of melting process (Table 2) and the eutectic transformation shares (u_k) of the total thermal effect obtained in the deconvolution process, the mass fractions of the phases involved in the eutectic transformation were determined according to Formula 2, with an uncertainty of measurement not exceeding 8 %. Figure 6 shows dependence of the experimental and calculated (Pandat) mass fractions of the transformed eutectic mixture on tin content, for both cross-sections with silver to copper molar ratios $X(Ag)/X(Cu) = 1$ and 7/3.

Differences between experimental and calculated values increase with decreasing tin content indicating the non-equilibrium excess of eutectic mixture in the tin composition range of the occurring earlier peritectic reaction. Excess amount of liquid, which is not fully reacted in the peritectic transformation according to the equilibrium
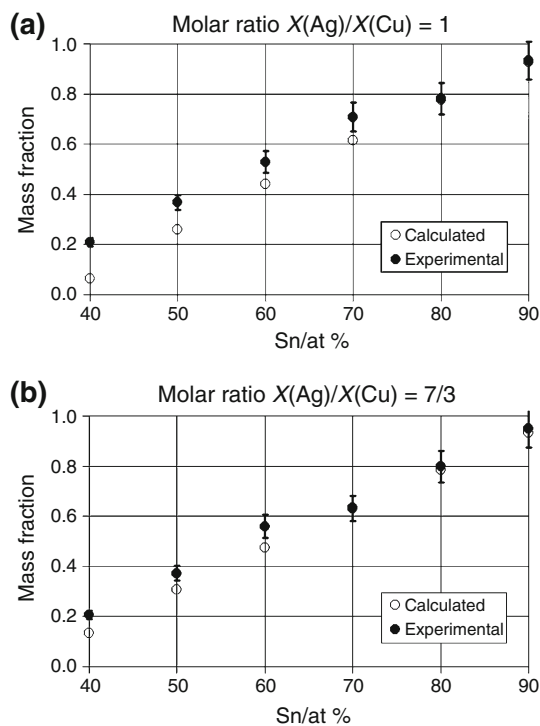
(a)

(b)

Fig. 6 Comparison of experimental (*full circles*) and calculated (*open circles*) (Pandat) changes of mass fractions of eutectics versus concentration of Sn, obtained for two cross-sections of molar ratios $X(Ag)/X(Cu) = 1$ and $7/3$

phase diagram, is ultimately solidified in the eutectic transformation, resulting in greater quantity of eutectics recorded by means of DSC measurements. Greater differences between the experimental and calculated results in the case of alloys with composition lying along $X(Ag)/X(Cu) = 1$ cross-section, may be due to a relatively lower efficiency of peritectic reaction, which is much faster ceased as a result of separation of liquid and consumed primary phase, which could grow earlier in a wider temperature range to a larger size.

Conclusions

Twelve compositions from Sn–Ag–Cu ternary system and eleven from Sn-Ag, Sn–Cu, and Ag–Cu alloys were studied by means of DSC. The determined temperatures of invariant reactions were compared with calculated phase diagrams of respective systems, which were calculated using the data from the COST 531 thermodynamic database. Good agreement is observed between the majority of experimentally determined invariant reactions and the results of calculations. Also, relatively good agreement is observed for alloys lying along $X(Ag)/X(Cu) = 1$ cross-section between our results and the data of Marianovic et al. [16].

The changes of mass fractions of phases involved in the eutectic transformation were determined with an uncertainty of measurement not exceeding 8 % and compared with values calculated using Pandat. A good agreement was observed for compositions of 80 and 90 at% of Sn (cross-section $X(Ag)/X(Cu) = 1$) and 70, 80, and 90 at% of Sn (cross-section $X(Ag)/X(Cu) = 7/3$). For the remaining alloys with relatively low Sn contents, the obtained values are higher, indicating a greater quantity of reacted eutectics compared with predicted values. These are compositions for which the initial matrix structure of alloys under DSC investigations contains structural effects of peritectic transformation. Greater differences between the experimental and calculated results in the case of alloys with composition lying along $X(Ag)/X(Cu) = 1$ cross-section, may be due to a relatively lower efficiency of peritectic reaction using phase (Cu_3Sn), which could grow earlier in a wider temperature range to a larger size. Under certain conditions, obtained results can be used to determine the amount of the phases involved in the eutectic transformation without having to know their usually unknown temperature-dependent densities, in contrast to the methods of quantitative metallography using measurements of volume fraction.

References

1. Espiritu R, Amorsolo A. DSC analysis of Cu–Zn–Sn shape memory alloy fabricated via electrodeposition route. J Therm Anal Calorim. 2012;107(2):483–7. doi:10.1007/s10973-011-1465-1.
2. Daoudi MI, Triki A, Redjaimia A. DSC study of the kinetic parameters of the metastable phases formation during non-isothermal annealing of an Al–Si–Mg alloy. J Therm Anal Calorim. 2011;104(2):627–33. doi:10.1007/s10973-010-1099-8.
3. Miller CM, Anderson IE, Smith JF. A viable tin-lead solder substitute: Sn–Ag–Cu. J Electron Mater. 1994;23:595–601.
4. Matsumoto T, Nogi K. Wetting in soldering and microelectronics. Annu Rev Mater Res. 2008;38:251–73.
5. Moon KW, Boettinger WJ, Kattner UR, Biancanielio FS, Handwerker CA. Experimental and thermodynamic assessment of Sn–Ag–Cu solder alloys. J Electron Mater. 2000;29:1122–36.
6. Loomans ME, Fine ME. Tin–silver–copper eutectic temperature and composition. Metall Mater Trans A. 2000;31A:1155–62.
7. Nishikawa H, Hamada Y, Takemoto T. Estimation method for liquidus temperature of lead-free solders using differential scanning calorimetry profiles. J Electron Mater. 2009;38:2610–6.
8. Moon KW, Boettinger WJ. Accurately determining eutectic composition: the Sn–Ag–Cu ternary eutectic. JOM J Miner Met Mater Soc. 2004;56(4):22–7.

9. Sopousek J, Pacult M, Hodulova E, Janovec J. Thermal analysis of the Sn–Ag–Cu–In solder alloy. J Electron Mater. 2010;39:312–7.

10. Park JY, Kim CU, Carper T, Pulugandla V. Phase equilibria studies of Sn–Ag–Cu eutectic solder using differential cooling of Sn–3.8Ag–0.7Cu alloys. J Electron Mater. 2003;32:1297–302.

11. Ohnuma I, Miyashita M, Anzai K, Liu XJ, Ohtani H, Kainuma R, Ishida K. Phase equilibria and the related properties of Sn–Ag–Cu based Pb-free solder alloys. J Electron Mater. 2000;29:1137–44.

12. Chen SW, Lin CC, Chen CM. Determination of the melting and solidification characteristics of solders using differential scanning calorimetry. Metall Mater Trans A. 1998;29A:1965–72.

13. Palcut M, Sopousek J, Trnkova L, Hodulova E, Szewczykova B, Ozvold M, Turn M, Janovec J. Thermal analysis of selected tin-based lead-free solder alloys. Kovove Mater. 2009;47:43–50.

14. Lee HM, Yoon SW, Lee BJ. Thermodynamic prediction of interface phases at Cu/solder joints. J Electron Mater. 1998;27:1161–6.

15. Chada S, Laub W, Fournelle RA, Shangguan D. An improved numerical method for predicting intermetallic layer thickness developed during the formation of solder joints on Cu substrates. J Electron Mater. 1999;28:1194–202.

16. Marianovic S, Manasijevic D, Minic D, Zivkovic D, Todorovic D. Thermal analysis of some alloys in the Ag–Cu–Sn ternary system. J Optoelectron Adv Mater. 2009;11(2):175–9.

17. Dinsdale AT, Watson A, Kroupa A, Zemanova A, Vrestal J, Vidal J, SOLDERS Database for Lead Free Solders. http://www.npl.co.uk/science-technology/advanced-materials/materials-areas/thermodynamics/thermodynamic-databases-for-mtdata. Accessed 29 Feb 2012.